Inorganic Chemistry

ARTICLE

pubs.acs.org/IC

Anion-Induced Structures and Luminescent Properties of Chiral Lanthanide−Organic Frameworks Assembled by an Achiral Tripodal Ligand

Xuhuan Yan,[†] Zhenghong Cai,[†] Chunli Yi, Weisheng Liu, Minyu Tan, and Yu Tang*

Key Laboratory of Nonferrous Metal Chemistry and Resources Utilization of Gansu Province, State Key Laboratory of Applied Organic Chemistry and College of Chemistry and Chemical Engineering, Lanzhou University, Lanzhou, 730000, P. R. China

Supporting Information

ABSTRACT: To confirm how different anions influence supramolecular self-assembly of lanthanide−organic frameworks (LnOFs) as well as their luminescent properties, a new flexible achiral tripodal ligand, 1,1,1-tris-{[(2′-benzylaminoformyl)-phenoxyl]methyl}ethane (L) and the LnOFs $\{[EuL(NO_3)_3]\cdot 1.5CHCl_3\}_n$ and $[EuL(pic)_3]_n$ have been designed and assembled. In the two LnOFs, $\{[EuL(NO_3)_3]\cdot 1.5CHCl_3\}_n$ demonstrates an unprecedented chiral noninterpenetrated two-dimensional (2D) honeycomblike (6,3) (hcb, Schläfli symbol 6^3, vertex symbol $6\cdot6\cdot6$) topological network, and $[EuL(pic)_3]_n$ confirms an unusual chiral LnOF with three-dimensional (3D) (10,3)-a (srs, $SrSi_2$, Schläfli symbol 10^3, vertex symbol $10_2\cdot10_4\cdot10_4$) topological framework. Also the anion-induced structures and energy transfer processes in the luminescence behavior of the two LnOFs were discussed in detail.

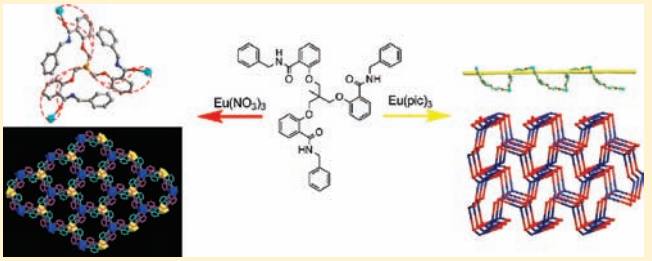

INTRODUCTION

During the past decade, increasing attention has been paid to the construction of chiral metal−organic frameworks (MOFs) due to their diverse applications in enantioselective separation, chiral catalysis, nonlinear optics, biomimetic chemistry, and magnetic materials.[1] One principle for constructing chiral MOFs is to select flexible ligands reasonably, because flexible ligands are labile and sensitive to the configuration environment. On the other hand, lanthanide centers with high coordination numbers and more variable nature of the coordination sphere have recently attracted the intense attention of crystal engineers, owing to their unique molecular architectures and fascinating chemical/physical properties. The approaches which have been reported previously on assembling chiral materials include the introduction of chiral ligands or chiral templates, the influence of the chiral physical environment, and spontaneous resolution which was induced by local distortion of the achiral organic ligand during the assembly process.[2] Usually, spontaneous resolution of chiral complexes without any chiral auxiliary is a peculiar phenomenon and has been found only occasionally in self-assembly of the MOFs. In this report, two anion-induced chiral lanthanide−organic frameworks (LnOFs) with (6,3) and (10,3)-a topological networks via spontaneous resolution were designed and assembled.

Until now, most of the work about (6,3) and (10,3)-a chiral networks have mainly focused on the transition metal-based metal−organic frameworks (MOFs).[3] However, the analogous chemistry of the lanthanide ions remain less developed.[4] The chiral MOFs having (6,3) and (10,3)-a topological frameworks can be targeted and constructed through direct assembly of triconnected inorganic and organic molecular building blocks (MBBs), so the triconnected flexible tripodal ligands are excellent candidates, which are labile and sensitive to the configuration environment including anions and solvent molecules. Taking these into consideration, a flexible amide type achiral tripodal ligand, 1,1,1-tris-{[(2′-benzylaminoformyl)phenoxyl]methyl}-ethane (L) (Scheme 1) was designed. The anion-induced structures and luminescent properties of the chiral (6,3) and (10,3)-a LnOFs assembled by lanthanide nitrate and picrate with L were also investigated. The crystal structure of $\{[EuL(NO_3)_3]\cdot 1.5CHCl_3\}_n$ demonstrates an unprecedented chiral noninterpenetrated 2D honeycomblike (6,3) topological network in lanthanide complexes, which is different from the previous 3D chiral honeycomblike open-framework constructed from lanthanide consolidating thiogallate-*closo*-dodecaborate $(K_3I)[SmB_{12}(GaS_4)_3]$ reported by Guo et al.[5] However, the structure of $[EuL(pic)_3]_n$ confirms an unusual chiral LnOF with a (10,3)-a topology net under the control of the picrate anion, which have previously been reported by us and Mao et al.[4] The anion-induced energy transfer processes in the luminescence behavior of the two LnOFs were also discussed in detail.

Received: October 11, 2010
Published: February 07, 2011

Scheme 1. Synthetic Route for the Ligand L

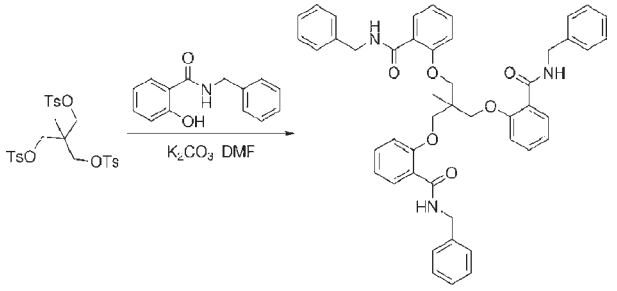

EXPERIMENTAL SECTION

Materials and Instrumentation. Lanthanide oxides (A. R.) were purchased from Shanghai Yuelong Co. Lanthanide nitrate was prepared by the reaction of lanthanide oxides and nitric acid (7 mol·L^{-1}), then superfluous nitric acid was removed. Lanthanide picrate[6] (***Caution!*** *Although we have experienced no problems in handling picrate compounds, these should be handled with great caution due to the potential for explosion.*), 1,1,1-Tris(*p*-tosyloxymethyl)ethane[7] and *N*-benzylsalicylamide[8] were prepared according to the literature methods. Other chemicals were obtained from commercial sources and purified by standard methods. C, H, and N were determined using an Elementar Vario EL elemental analyzer. The IR spectra were recorded in the 4000−400 cm^{-1} region using KBr pellets and a Nicolet Nexus 670 FT-IR instrument. ^{1}H NMR spectra were recorded at 400 MHz and ^{13}C NMR spectra at 100 MHz with Bruker Avance 400 spectrometer in $CDCl_3$ solutions, with tetramethylsilane ($Si(CH_3)_4$) as an internal standard. UV/vis absorption spectra were determined on a Varian UV-Cary100 spectrophotometer. The steady-state luminescence spectra and the lifetime measurements were measured on an Edinburgh Instruments FSL920 fluorescence spectrometer, with 450 W Xe arc lamp as the steady-state excitation source or Nd-pumped OPOlette laser as the excitation source for lifetime measurements. Phosphorescence spectra were obtained on a Hitachi F-4500 fluorescence spectrophotometer.

Synthesis of the Ligand L. *N*-Benzylsalicylamide (3.4 g, 15 mmol), anhydrous potassium carbonate (2.5 g, 18.1 mmol), and dry dimethylformamide (25 cm^3) were warmed to ca. 90 °C and 1,1,1-tris(*p*-tosyloxymethyl)ethane (2.91 g, 5.0 mmol) was added. The reaction mixture was stirred at 90 °C for 12 h. After cooling down, the mixture was poured into water (200 cm^3). The resulted solid was treated by column chromatography on silica gel using petroleum-ethyl acetate (2:1) as eluent to get white solid L, yield 64%; mp 65−67 °C. Elemental analysis calcd. for $C_{47}H_{45}N_3O_6$: C, 75.48; H, 6.06; N, 5.62%. Found: C, 75.60; H, 6.24; N, 5.65. IR (KBr, ν, cm^{-1}): 3410 (m, NH), 1646 (s, C═O), 1602 (m), 1536 (m), 1489 (m), 1452 (m), 1297 (m), 1229 (s), 1047 (m), 755 cm^{-1} (s). ^{1}H NMR (400 MHz, $CDCl_3$, 25 °C, $Si(CH_3)_4$) δ: 0.44 (s, 3H, CH_3), 3.57 (s, 6H, OCH_3), 4.51 (d, J = 5.2 Hz, 6H, $NHCH_2$), 6.57 (d, J = 8 Hz, 3H, Ar), 7.07−7.16 (m, 18H, Ar), 7.26−7.32 (t, 3H, Ar), 7.39−7.43 (dd, 3H, Ar), 8.15−8.18 (d, J = 8 Hz, 3H, −NH−). ^{13}C NMR (100 MHz, $CDCl_3$, 25 °C, $Si(CH_3)_4$) δ: 16.96, 39.52, 44.31, 71.19, 112.26, 122.09, 122.21, 127.74, 128.45, 128.75, 132.21, 132.77, 137.86, 155.42, 164.90.

Synthesis of Lanthanide Nitrate and Picrate Complexes. A solution of 0.10 mmol L in 10 cm^3 of chloroform was added dropwise to a solution of 0.10 mmol $Eu(NO_3)_3·6H_2O$, $Gd(NO_3)_3·6H_2O$, or $Eu(pic)_3·6H_2O$ in 10 cm^3 of ethyl acetate. The mixture was stirred at room temperature for 4 h. The precipitated solid complex was filtered, washed with ethyl acetate/chloroform, and dried in vacuo over P_4O_{10} for 48 h and submitted for elemental analysis, yield 64−75%. Elemental analytical and IR spectral data for the complexes are summarized in Table 1.

X-ray Crystallographic Study. The X-ray single-crystal data collections were performed at room temperature on a Bruker Smart 1000 CCD diffractometer, using graphite-monochromated Mo $K\alpha$ radiation (λ = 0.71073 Å). Semiempirical absorption corrections were applied using the SADABS program. The structures were solved by direct methods and refined by full-matrix least-squares on F^2 using the SHELXS-97 and SHELXL-97 programs.[9] Anisotropic thermal parameters were assigned to all non-hydrogen atoms. The hydrogen atoms were set in calculated positions and refined as riding atoms with a common fixed isotropic thermal parameter. Analytical expressions of neutral atom scattering factors were employed, and anomalous dispersion corrections were incorporated. The crystal data and refinement results are summarized in Table 2. Selected bond lengths and angles of $\{[EuL(NO_3)_3]·1.5CHCl_3\}_n$ and $[EuL(pic)_3]_n$ are given in Supporting Information Tables S1 and S2, respectively. Hydrogen bonds in crystal packing for the compounds $\{[EuL(NO_3)_3]·1.5CHCl_3\}_n$ and $[EuL(pic)_3]_n$ are listed in Supporting Information Tables S3 and S4. CCDC 776154 ($\{[EuL(NO_3)_3]·1.5CHCl_3\}_n$) and 248592 ($[EuL(pic)_3]_n$) contain the supplementary crystallographic data for this paper. These data can be obtained free of charge from The Cambridge Crystallographic Data Centre via www.ccdc.cam.ac.uk/data_request/cif.

Table 1. Elemental Analytical and IR Spectral Data of the Complexes

	found (calcd.) %			IR (cm^{-1})
compounds	C	H	N	ν(C═O)
$EuL(NO_3)_3$	51.76 (51.99)	4.40 (4.18)	7.45 (7.44)	1609
$GdL(NO_3)_3·2H_2O$	50.46 (50.08)	4.02 (4.38)	7.45 (7.46)	1609
$EuL(pic)_3·H_2O$	48.71 (48.73)	3.19 (3.33)	10.48 (10.49)	1613

RESULTS AND DISCUSSION

Synthesis and General Characterization. Amide type tripodal ligands have the advantage of the selective coordinating capacity and hard binding sites, therefore stabilizing their complexes, acquiring new coordination structures and shielding the encapsulated lanthanide ions from interaction with the surroundings, and thus to exhibit good luminescent properties. Ligand 1,1,1-tris-{[(2′-benzylaminoformyl)phenoxyl]methyl}ethane (L) was prepared by the ether base coupling of 1,1,1-tris(*p*-tosyloxymethyl)ethane and the appropriate *N*-benzylsalicylamide in a 1:3 ratio in dry DMF in the presence of an excess of anhydrate K_2CO_3. The resulted solid was treated by column chromatography on silica gel using petroleum-ethyl acetate (2:1) as eluent to get white solid L, yield 64%. The ligand gave satisfactory ^{1}H NMR, ^{13}C NMR, and IR spectra and elemental analysis. Treatment of $Eu(NO_3)_3·6H_2O$, $Gd(NO_3)_3·6H_2O$, and $Eu(pic)_3·6H_2O$ with the ligand in ethyl acetate−chloroform mixed solution yielded three complexes which, according to the elemental analysis, correspond to the formula of $EuL(NO_3)_3$, $GdL(NO_3)_3·2H_2O$, and $EuL(pic)_3·H_2O$, respectively. The solid powder of the complexes $EuL(NO_3)_3$ and $GdL(NO_3)_3·2H_2O$ are soluble in DMF, DMSO, methanol, ethanol, and acetone, slightly soluble in acetonitrile, but insoluble in $CHCl_3$ and diethyl ether. The complex $EuL(pic)_3·H_2O$ is soluble in DMF, DMSO, slightly soluble in methanol, ethanol, and acetone, but insoluble in $CHCl_3$, acetonitrile, and diethyl ether. The IR spectrum of the free ligand displays characteristic absorption of carbonyl group at 1646 cm^{-1}. Compared to the free ligand, the absence of the band 1646 cm^{-1}, which is instead by a new band at ca. 1610 cm^{-1} of the complexes, indicates that the oxygen atom of the carbonyl group takes part in coordination to the metal ion. After several weeks of slow evaporation of the ethyl

dx.doi.org/10.1021/ic102033d |*Inorg. Chem.* 2011, 50, 2346–2353

Table 2. Crystal Data and Structure Refinements for the LnOFs $\{[EuL(NO_3)_3]\cdot 1.5CHCl_3\}_n$ and $[EuL(pic)_3]_n$

complex	$\{[EuL(NO_3)_3]\cdot 1.5CHCl_3\}_n$	$[EuL(pic)_3]_n$
empirical formula	$C_{48.50}H_{46.50}Cl_{4.50}EuN_6O_{15}$	$C_{65}H_{51}EuN_{12}O_{27}$
formula weight	1264.90	1584.14
temperature (*K*)	293(2)	293(2)
wavelength (Å)	0.71073	0.71073
crystal system	hexagonal	cubic
space group	$P6_3$ (no. 173)	$P2_13$ (no. 198)
a (Å)	13.528(2)	18.639(3)
c (Å)	17.410(3)	18.639(3)
volume (Å^3)	2759.4(8)	6475(2)
Z	2	4
D_{calcd} (g cm^{-3})	1.522	1.625
μ (Mo Kα) (mm^{-1})	1.424	1.068
F (000)	1278	3216
crystal size (mm)	0.48 × 0.40 × 0.37	0.47× 0.45 × 0.20
range (deg)	2.10−25.01	1.89−25.98
index ranges	$-14 \le h \le 16$, $-16 \le k \le 16$ $-20 \le l \le 20$	$-22 \le h \le 22$, $-22 \le k \le 20$ $-19 \le l \le 22$
reflection collected	14212	39165
independent reflections	3191[(R_{int}) = 0.0388]	4244[(R_{int}) = 0.0291]
data/restraints/parameters	3191/536/230	4244/2/317
goodness-of-fit on F^2	1.066	1.039
final *R* indices	R_1 = 0.0499, wR_2 = 0.1294	R_1 = 0.0254, wR_2 = 0.0672
R indices (all data)	R_1 = 0.0654, wR_2 = 0.1429	R_1 = 0.0282, wR_2 = 0.0688

acetate/chloroform/methanol solutions, the crystals suitable for X-ray analysis of the europium nitrate and picrate complexes were obtained.

Crystal Structure Descriptions. *Crystal Structure of $\{[EuL(NO_3)_3]\cdot 1.5CHCl_3\}_n$.* The crystal analysis unambiguously reveals that $\{[EuL(NO_3)_3]\cdot 1.5CHCl_3\}_n$ crystallizes in the hexagonal chiral space group $P6_3$ and possesses a chiral porous 2D honeycomb open framework. The assembly of a honeycomblike structure is challenging since the hexagon represents the most common pattern in nature and is familiar from benzene to the honeycomb of the bee. To the best of our knowledge, this is the first example of the neutral chiral noninterpenetrated (6,3) (hcb, Schläfli symbol 6^3, vertex symbol 6·6·6) topological LnOF. Careful structural analysis reveals that the LnOF $\{[EuL(NO_3)_3]\cdot 1.5CHCl_3\}_n$ has crystallographic C_3 symmetry. So, an asymmetric unit contains 1/3 Eu^{3+}, 1/3 ligand, 1 nitrate, and 1/2 chloroform molecules. As shown in Figure 1a, each Eu^{3+} ion is coordinated with nine oxygen donor atoms, among which six oxygen atoms belong to three bidentate nitrate groups (O3, O4) and the remaining three are from carbonyl groups of three tripodal ligands (O2). The Eu^{3+} center lies in a distorted tricapped trigonal prism coordination environment (Figure 1b). The Eu−O (nitrate) distances are between 2.437(8) and 2.554(6) Å, and the Eu−O (carbonyl) bond length is 2.364(7), both of which are comparable to the corresponding Eu−O bond lengths found in related complexes.[10] At the same time, each ligand binds to three Eu^{3+} using its three oxygen atoms of the amide groups. So each Eu^{3+} connects with three ligands, meanwhile, each ligand connects with three Eu^{3+} ions despite the existence of the coordinated nitrate groups, thus the Eu^{3+} ion and the ligand L can be treated as three connected building units, which form a 1:1 LnOF. Thus, the whole structure consists of an infinite array of trigonal Eu^{3+} ions bridged by tridentate ligands, and a $(ML)_3$ type 2D honeycomblike topological net is formed (Figure 1c). The six-membered rings composed of Eu^{3+} centers, and tripodal ligands in the sheet are all in a chairlike structure. The sheets are stacked in an AB sequence along the crystallographic *c*-axis (Figure 1d). In addition, the coordination layers are linked by intermolecular hydrogen bonds O···H−C to form a 3D netlike supermolecule. The ligands themselves with large terminal groups and $CHCl_3$ molecules fill the void in the channels and thus prevent self-interpenetration. Calculation using PLATON[11] reveals that the solvent-accessible portion accounts for about 19.9% of the crystal volume. Besides, all the anions do not lie in cavities within the network but bind to the Eu^{3+}, so the whole frame is a completely neutral network. The chirality of the framework results from the flexibility of the amide type tripodal ligand with three freely rotatable salicylamide moieties. The ligand connects with three Eu^{3+} with its three carbonyl groups in an anticlockwise propeller fashion (Figure 1e), and a C_3 symmetry is imposed, thus endowing intrinsic chirality.

Crystal Structure of $[EuL(pic)_3]_n$. To confirm the role of different anions in the self-assembly process, picrate with a larger size was used instead of nitrate to perform the reaction. The single-crystal X-ray analysis reveals that the compound $[EuL(pic)_3]_n$ belongs to the cubic chiral space group $P2_13$ and has crystallographic C_3 symmetry. An asymmetric unit contains 1/3 Eu^{3+}, 1/3 ligand, and 1 picrate anion. As shown in Figure 2a, each Eu^{3+} is coordinated with six oxygen donor atoms from three bidentate picrate groups (O3, O9) and three to carbonyl groups from three tripodal ligands (O2). The coordination polyhedron around Eu^{3+} is a distorted tricapped trigonal prism (Figure 2b). The Eu−O (picrate) bond lengths span the range of 2.339(2)−2.631(2) Å, and the Eu−O (carbonyl) bond lengths is 2.402(2), both of which are comparable to the corresponding Eu−O bond lengths found in related complexes.[10] At the same time, each ligand binds to three Eu^{3+} using its three oxygen atoms of the amide groups. Thus, the whole structure consists of an infinite array of trigonal Eu^{3+} bridged by tridentate ligands, and a 3D coordination polymer is formed (Figure 2c). A better insight into the nature of the involved framework can be achieved by the application of a topological approach. The ligand L and Eu^{3+} were assembled to a desired chiral LnOF having (10,3)-a (srs, $SrSi_2$, Schläfli symbol 10^3, vertex symbol $10_2\cdot 10_4\cdot 10_4$) topology (three connections to each point and shortest closed circuit containing ten points) (Figure 2d). There are seven uniform (10,3) connected nets as described by Wells,[12] characteristic features of single (10,3)-a net are 4-fold helices (four links per turn), all of the same handness, running parallel to the cubic cell edges; therefore, the network is chiral. In contrast to its prototypal frame, this complex contains two types of alternating centers, so that the original interconnected 4_1 helical chains become 2_1 Eu−L−Eu−L helixes with the helical distance 18.639 Å, which happen to be right-handed (Figure 2e). In addition, the entire picrates bind to the Eu^{3+}, so the whole frame is a completely neutral network, and the ligands fill the channels themselves with their "thick" rods and large terminal groups and thus prevent self-interpenetration. The volume of cavities calculated by PLATON[11] is 2.6%. To the best of our knowledge, the compound $[EuL(pic)_3]_n$ is a rare example of a (10,3)-a network that is neutral and noninterpenetrated.

dx.doi.org/10.1021/ic102033d |*Inorg. Chem.* 2011, 50, 2346–2353

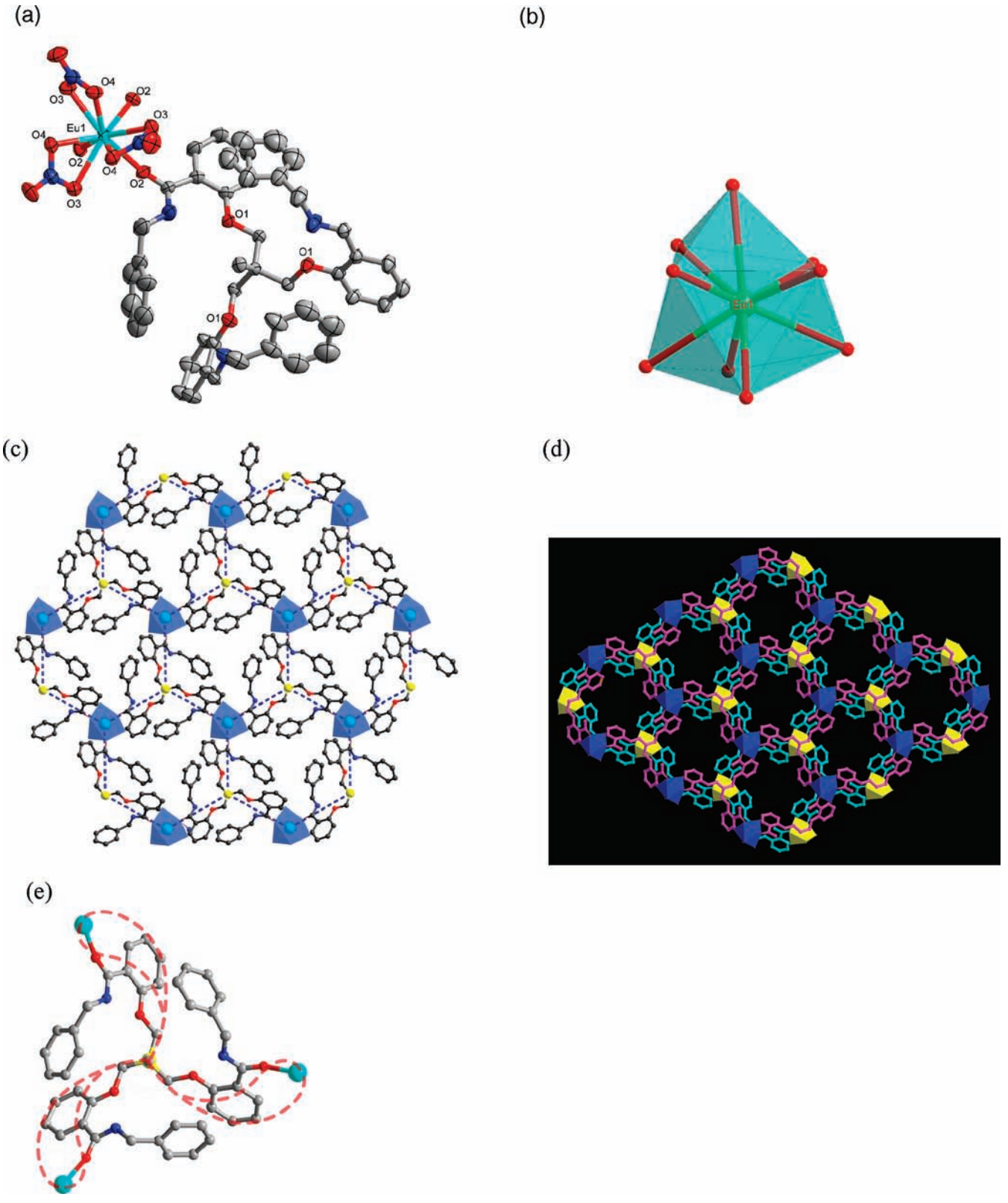

Figure 1. (a) Local coordination environment of Eu^{3+} in LnOF $\{[EuL(NO_3)_3]\cdot 1.5CHCl_3\}_n$ with thermal ellipsoids at 30% probability. (b) Coordination polyhedron of Eu^{3+}. (c) View of the 2D honeycomb (6,3) net structure of the compound $\{[EuL(NO_3)_3]\cdot 1.5CHCl_3\}_n$ in the *ab* plane. (d) View of 3D noninterpenetrated honeycomblike layers of (6,3) topology with 1D channels along the *c*-axis. The 2D layer architectures of the LnOF $\{[EuL(NO_3)_3]\cdot 1.5CHCl_3\}_n$ are stacked in AB sequence along the crystallographic *c*-axis. (e) Partial molecular structure of (6,3) net and chirality of the propellerlike structure (hydrogen atoms, $CHCl_3$ molecules; all nitrates and benzylamine groups of the ligands are omitted for clarity).

dx.doi.org/10.1021/ic102033d |*Inorg. Chem.* 2011, 50, 2346–2353

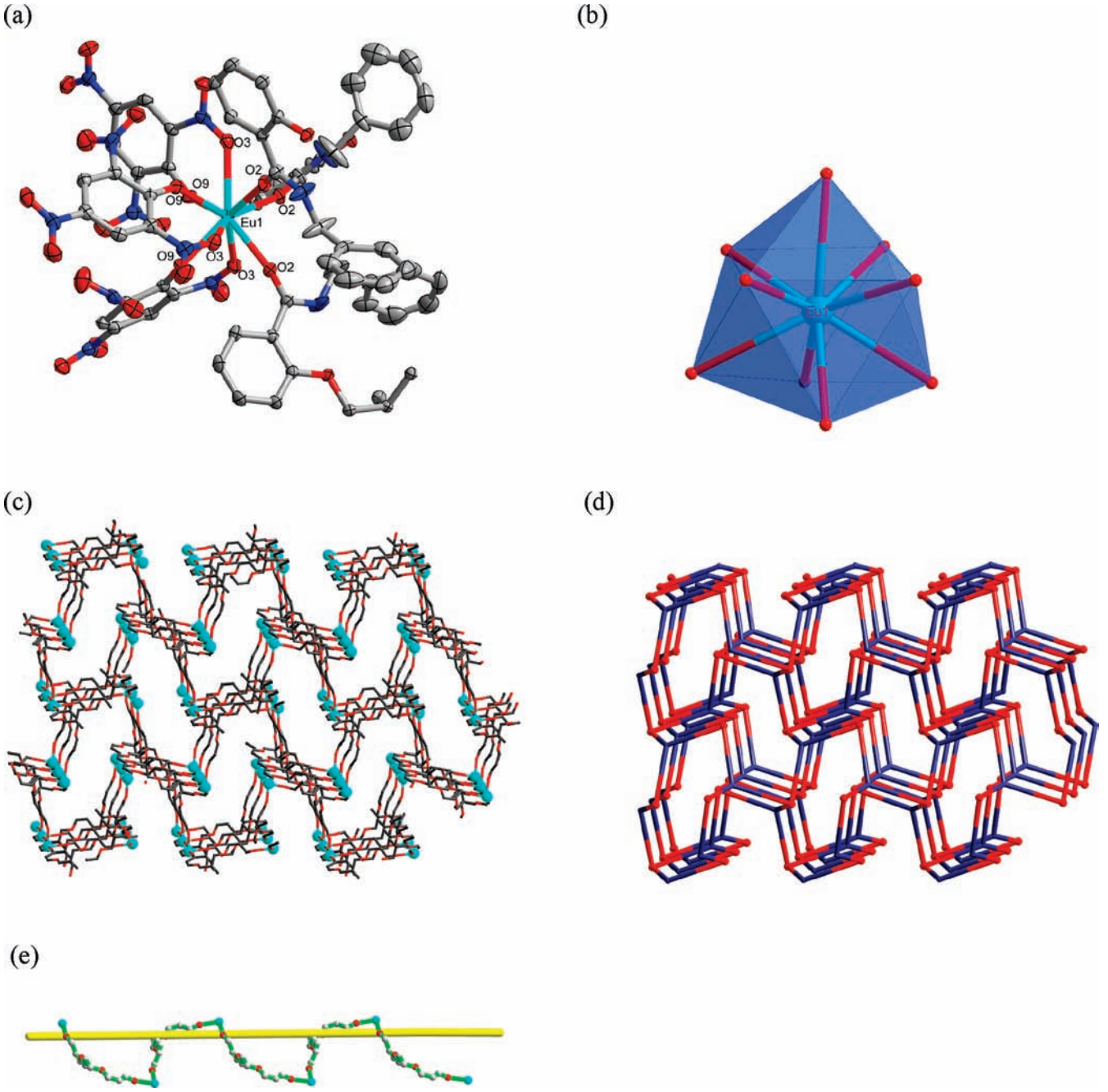

Figure 2. (a) Local coordination environment of Eu^{3+} in LnOF $[EuL(pic)_3]_n$ with thermal ellipsoids at 30% probability. (b) Coordination polyhedron of Eu^{3+}. (c) Simplified crystal unit packing arrangement of the compound $[EuL(pic)_3]_n$. (All hydrogen atoms, nitrates, benzene rings of branched chain, and benzylamine groups of the ligands are omitted for clarity.) (d) Schematic representation of the (10,3)-a topological framework of compound $[EuL(pic)_3]_n$ as viewed along the *a*-axis. Red nodes represent the Eu^{3+} centers, and blue nodes represent the anchors of the ligands. (e) Schematic illustration of the carbonyl−europium chains in compound $[EuL(pic)_3]_n$ propagating along the *a*-axis. The yellow rod is the crystallographic 2_1 screw axis (right-handed).

Comparison of the Structures. In the investigations of the self-assembly between $Eu(NO_3)_3 \cdot 6H_2O$, $Eu(pic)_3 \cdot 6H_2O$, and the ligands, calculation performed using PLATON[11] reveals that the nitrates and picrates account for about 9.1 and 39.0% of the crystal volume, respectively. We speculate that the most important factor which results in the difference in structures of $\{[EuL(NO_3)_3] \cdot 1.5CHCl_3\}_n$ and $[EuL(pic)_3]_n$ is effective space filling of the network voids/channels by picrates, which leads to the formation of a noninterpenetrated (10,3)-a net instead of (6,3) topological framework.[13] A deeper view of the LnOF $\{[EuL(NO_3)_3] \cdot 1.5CHCl_3\}_n$ indicates that the dihedral angle between the plane formed by three O1 of tripodal ligand and the plane formed by three O2 (C═O) which bind to Eu^{3+} is 0°; however, in the LnOF $[EuL(pic)_3]_n$, the dihedral angle is 70.53°, which is consistent with the ideal angle (0°) to form a (6,3) net and very close to the ideal one (71°) to form a (10,3)-a

dx.doi.org/10.1021/ic102033d |*Inorg. Chem.* 2011, 50, 2346–2353

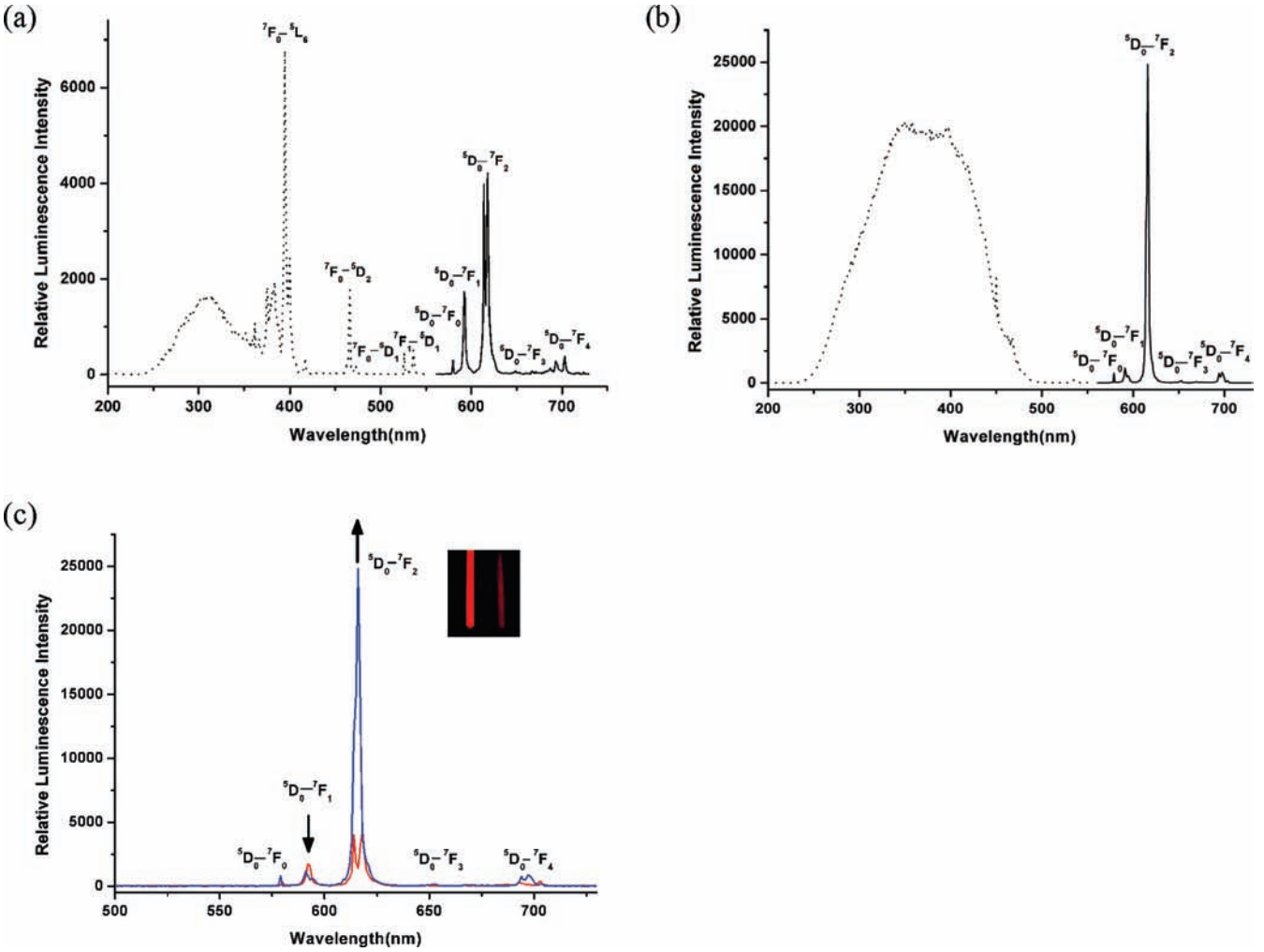

Figure 3. (a) Room-temperature excitation with emission monitored at approximately 618 nm and emission spectra for the compound $\{[EuL(NO_3)_3]\cdot 1.5CHCl_3\}_n$ (λ_{ex} = 396 nm, excitation and emission slits are 0.10 nm) in the solid state. (b) Room-temperature excitation with emission monitored at approximately 616 nm and emission spectra for the compound $[EuL(pic)_3]_n$ (λ_{ex} = 398 nm, excitation and emission slits are 0.10 nm) in the solid state. (c) Room-temperature emission spectra for the compounds $\{[EuL(NO_3)_3]\cdot 1.5CHCl_3\}_n$ and $[EuL(pic)_3]_n$. (inset) Color changes for compounds $[EuL(pic)_3]_n$ (left) and $\{[EuL(NO_3)_3]\cdot 1.5CHCl_3\}_n$ (right) under the excitation of UV light (λ_{ex} = 365 nm).

network.[14] The porosity is a very important property for coordination polymers; however, many obtained porous structures are often accompanied with interpenetration, thus influencing the applications of the porous property. Until now, many reported (10,3)-a net structures are interpenetrated.[3i−3m] It is noteworthy that the chiral LnOFs reported here are non-interpenetrated. However, unfortunately, the ligands fill the channels themselves with their thick rods and large terminal groups. It seems like a contradiction. So there is much to do to find well-designed molecular materials with large channels or holes.

Luminescent Properties of the LnOFs. The solid state luminescent properties of the nitrate and picrate salts of the LnOFs were examined at room temperature, and the excitation spectrum of $\{[EuL(NO_3)_3]\cdot 1.5CHCl_3\}_n$ (Figure 3a) has negligible contribution from the ligand and exhibits a series of sharp lines characteristic of the Eu^{3+} energy-level structure, which can be assigned to transitions between the $^7F_{0,1}$ and $^5L_6$, $^5D_{2,1}$ levels.[15] This indicates that the Eu^{3+} luminescence is not efficiently sensitized by the ligand. The excitation and emission spectra of $[EuL(pic)_3]_n$ are shown in Figure 3b. The excitation spectrum exhibits a broad excitation band (BEB) between 250 and 500 nm. The broad excitation band in the excitation spectrum could be primarily assigned to the $\pi-\pi^*$ electron transition of the picrate anion, because the compounds $Eu(pic)_3\cdot 6H_2O$ and $[EuL(pic)_3]_n$ have similar absorption bands (Figure S1, Supporting Information). The peak at 467 nm in the excitation spectrum of $[EuL(pic)_3]_n$ can be ascribed to the f−f transition ($^7F_0 \rightarrow {}^5D_2$) of Eu^{3+} ion, which is overlapped by BEB, proving that the luminescence sensitization via excitation of the picrates is more efficient than the direct excitation of the Eu^{3+} ions absorption level. The emission spectra of the solid state $Eu(NO_3)_3\cdot 6H_2O$, $\{[EuL(NO_3)_3]\cdot 1.5CHCl_3\}_n$, $Eu(pic)_3\cdot 6H_2O$, and $[EuL(pic)_3]_n$ (Figure S2, Supporting Information) show that when the ligand is coordinated with Eu^{3+}, the luminescence intensities of $Eu(NO_3)_3\cdot 6H_2O$ and $Eu(pic)_3\cdot 6H_2O$ are obviously enhanced. We speculate that coordinated water molecules existing in the compounds serve as efficient oscillators for the Eu^{3+} luminescence emission in $Eu(NO_3)_3\cdot 6H_2O$ and $Eu(pic)_3\cdot 6H_2O$. The replacement of water by the ligand molecules in the coordination sphere reduce the quenching efficiency,[16] and meanwhile, organic ligand molecules can be considered as antennae and

dx.doi.org/10.1021/ic102033d |*Inorg. Chem.* 2011, 50, 2346–2353

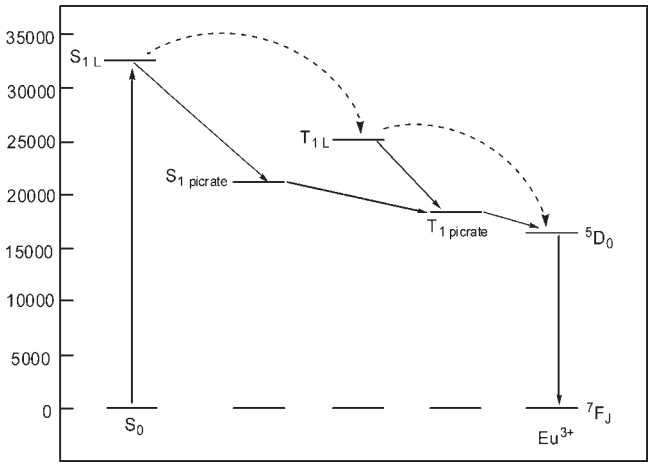

Figure 4. Schematic energy level diagram and the energy transfer process: S_1, first excited singlet state; T_1, first excited triplet state.

transfer energy to Eu^{3+}. As a result, the luminescence intensity is greatly enhanced.

The emission spectra of the nitrate and picrate salts of the LnOFs reveal five characteristic peaks of Eu^{3+} which are attributed to $^5D_0 \rightarrow {}^7F_0$ (580 nm), $^5D_0 \rightarrow {}^7F_1$ (592 nm), $^5D_0 \rightarrow {}^7F_2$ (616 nm), $^5D_0 \rightarrow {}^7F_3$ (650 nm), and $^5D_0 \rightarrow {}^7F_4$ (693 nm). The intensities of the $^5D_0 \rightarrow {}^7F_2$ transition (electric dipole) are stronger than those of the $^5D_0 \rightarrow {}^7F_1$ transition (magnetic dipole), indicating that the coordination environment of the Eu^{3+} ions is asymmetric,[17] which is consistent with the crystallographic analysis. Replacement of the nitrate anion with the picrate anion not only resulted in structural changes dramatically but also in luminescent properties of the LnOFs enormously. For $[EuL(pic)_3]_n$, the emission intensity of the $^5D_0 \rightarrow {}^7F_2$ transition is approximately 6 times stronger than that of $\{[EuL(NO_3)_3]\cdot 1.5CHCl_3\}_n$ under the same conditions; however, the emission intensity of the $^5D_0 \rightarrow {}^7F_1$ transition is only an estimated 0.85 times (Figure 3c). The increased monochrome of the picrate salt of the LnOF may be applied to design new luminous materials. To our knowledge, there are few examples of this kind of luminescence effect,[18] which needs further investigation. Following the method described in the literature,[19] it is possible to estimate the $^5D_0$ quantum efficiency (q) of the complexes on the basis of the luminescence data (emission spectra and $^5D_0$ lifetimes, Figures S3 and S4, Supporting Information). The emission quantum efficiencies evaluated for $\{[EuL(NO_3)_3]\cdot 1.5CHCl_3\}_n$ and $[EuL(pic)_3]_n$ are 31.79 and 39.59% (Table S5, Supporting Information), respectively.

Energy Transfer Processes Studies. It is well-known that the neutral ligands often play a vital role of absorbing and transporting energy to the other ligands or the central metal ions in the lanthanide complexes.[20] We have investigated the energy transfer processes in order to elucidate why the luminescence intensity of the picrate salt of the LnOF is much higher than that of the nitrate salt of the LnOF. The triplet excited energy-level T_1 data of the ligand and picrate were calculated by the low-temperature (77 K) phosphorescence spectra of the compounds $GdL(NO_3)_3\cdot 2H_2O$ and $Gd(pic)_3\cdot 6H_2O$ in a 1:1 methanol−ethanol mixture (Figure S5, Supporting Information). Because the expected coordination environments for Gd^{3+} ion (radius 94 pm) and Eu^{3+} ion (radius 95 pm) are similar and the energy absorbed by the ligand and picrate could not be transferred to the lowest excited state of the Gd^{3+} ion (high to about 32 000 cm^{-1}), the triplet states of the ligand and picrate can be determined by the shortest-wavelength phosphorescence bands of the Gd^{3+} compounds.[21] The phosphorescence spectra demonstrated that the triplet energy levels (T_1) of ligand and picrate are 25 000 (400) and 18 248 cm^{-1} (548 nm), respectively, both of which are higher than the lowest excited state of the $^5D_0$ level of Eu^{3+} (17 267 cm^{-1}). The singlet state energy levels of ligand and picric acid are estimated by referencing their absorbance edges, which are 32 258 (310) and 21 505 cm^{-1} (465 nm), respectively (Figure S6, Supporting Information). In the nitrate salt of the LnOF $\{[EuL(NO_3)_3]\cdot 1.5CHCl_3\}_n$, we speculate that energy transfers from the S_1 to the T_1 excited state of the ligand and then transfers from the T_1 excited state of the ligand to the emitting level of Eu^{3+}. Because the energy gap between the ligand triplet and Eu^{3+} excited states (7733 cm^{-1}) is too large, the ligand cannot efficiently sensitize the Eu^{3+} luminescence. For compound $[EuL(pic)_3]_n$, the energy transfer process can be summarized in three approaches. Energy may transfer from the S_1 to the T_1 excited state of ligand and then transfer from the T_1 excited state of the ligand to the emitting level of Eu^{3+} ion directly; energy transfers from the S_1 excited state of the ligand to that of picrate and transfers from the S_1 to the T_1 excited state of picrate, then through the T_1 excited state of picrate to the emitting level of Eu^{3+}; or energy transfers from the S_1 to the T_1 excited state of the ligand, then through the T_1 excited state of picrate to the emitting level of Eu^{3+} (Figure 4). Because the triplet state of the ligand is much higher than the europium ion, which makes the energy transfer from ligand to the europium ion restricted, it can go through the triplet state of the picrate as the major pathway of the energy transfer.[22] Obviously, compared to the nitrate salt of the LnOF $\{[EuL(NO_3)_3]\cdot 1.5CHCl_3\}_n$, the picrate salt of the LnOF $[EuL(pic)_3]_n$ may have more additional energy transfer routines to improve the energy transfer efficiency from the ligand to the central ion.

CONCLUSION

In summary, we designed and synthesized a new achiral amide type tripodal ligand, 1,1,1-tris-{[(2′-benzylaminoformyl)phenoxyl]methyl}ethane (L). Furthermore, the first example of 2D chiral noninterpenetrated honeycomblike (6,3) topological network $\{[EuL(NO_3)_3]\cdot 1.5CHCl_3\}_n$ was found in the LnOFs. With the use of picrate anion instead of nitrate anion, the LnOF $[Eu(pic)_3L]_n$ with chiral noninterpenetrated 3D (10,3)-a network structure was assembled. We speculate that the significant factor which results in the variance between their structures is the different volume of anions. We also studied how different anions affect the luminescent properties of the LnOFs. The acquired LnOFs $\{[EuL(NO_3)_3]\cdot 1.5CHCl_3\}_n$ and $[EuL(pic)_3]_n$ both exhibit characteristic luminescence emissions of the Eu^{3+} in the visible band, and the luminescence intensity of the latter has a more dramatic enhancement compared with the former. The energy transfer processes indicate that the picrate salt of the LnOF may have more additional energy transfer routines than the nitrate salt of the LnOF, which might improve the energy transfer efficiency to the central ion. From a more general perspective, they have potential applications in the area of luminous materials, gas storage, separation, and catalysis.

■ ASSOCIATED CONTENT

Supporting Information. Materials and methods, tables of selected bond distances and angles, hydrogen bonds in crystal packing and photoluminescence data for the LnOFs $\{[EuL(NO_3)_3]\cdot 1.5CHCl_3\}_n$ and $[Eu(pic)_3L]_n$, absorption spectra of the ligand and picric acid, emission spectra for the compounds $Eu(NO_3)_3\cdot 6H_2O$, $\{[EuL(NO_3)_3]\cdot 1.5CHCl_3\}_n$, $Eu(pic)_3\cdot 6H_2O$, and $[Eu(pic)_3L]_n$, phosphorescence spectra of compounds $GdL(NO_3)_3\cdot 2H_2O$ and $Gd(pic)_3\cdot 6H_2O$, crystallographic data in CIF format. This material is available free of charge via the Internet at http://pubs.acs.org.

■ AUTHOR INFORMATION

Corresponding Author

*Tel.: +86-931-8912552. Fax: +86-931-8912582. E-mail address: tangyu@lzu.edu.cn.

Author Contributions

†These authors contributed equally to this work.

■ ACKNOWLEDGMENT

This work was financially supported by the National Natural Science Foundation of China (Project 20931003, 21071068) and the program for New Century Excellent Talents in University (NCET-06-0902).

■ REFERENCES

(1) (a) Férey, G. *Chem. Soc. Rev.* **2008**, *37*, 191. (b) Férey, G.; Mellot-Draznieks, C.; Serre, C.; Millange, F. *Acc. Chem. Res.* **2005**, *38*, 217. (c) Wu, C.; Hu, A.; Zhang, L.; Lin, W. *J. Am. Chem. Soc.* **2005**, *127*, 8940. (d) Mantion, A.; Massüger, L.; Rabu, P.; Palivan, C.; McCusker, L. B.; Taubert, A. *J. Am. Chem. Soc.* **2008**, *130*, 2517. (e) Ma, L.-Q.; Lin, W.-B. *J. Am. Chem. Soc.* **2008**, *130*, 13834. (f) Ma, L.; Abney, C.; Lin, W. *Chem. Soc. Rev.* **2009**, *38*, 1248. (g) Verbiest, T.; Elshocht, S. V.; Kauranen, M.; Hellemans, L.; Snauwaert, J.; Nuckolls, C.; Katz, T. J.; Persoons, A. *Science* **1998**, *282*, 913. (h) Kim, K.; Seo, J. S.; Whang, D.; Lee, H.; Jun, S. I.; Oh, J.; Jeon, Y. J. *Nature* **2000**, *404*, 982. (i) Lee, S. J.; Hu, A.; Lin, W. *J. Am. Chem. Soc.* **2002**, *124*, 12948. (j) Xiong, R.-G.; You, X.-Z.; Abrahams, B. F.; Xue, Z.-L.; Che, C.-M. *Angew. Chem., Int. Ed.* **2001**, *40*, 4422. (k) Kitagawa, S.; Kitaura, R.; Noro, S. *Angew. Chem., Int. Ed.* **2002**, *41*, 1159. (l) Lenoble, G.; Lacroix, P. G.; Daran, J. C.; Bella, S. D.; Nakatani, K. *Inorg. Chem.* **1998**, *37*, 2158.

(2) Qiu, S.-L.; Zhu, G.-S. *Coord. Chem. Rev.* **2009**, *253*, 2891.

(3) (a) Prior, T. J.; Bradshaw, D.; Teatb, S. J.; Rosseinsky, M. J. *Chem. Commun.* **2003**, 500. (b) Youm, K.-T.; Huh, S.; Park, Y.- J.; Park, S.; Choia, M.-G.; Jun, M.-J. *Chem. Commun.* **2004**, 2384. (c) Shestopalov, M. A.; Cordier, S.; Hernandez, O.; Molard, Y.; Perrin, C.; Perrin, A.; Fedorov, V. E.; Mironov, Y. V. *Inorg. Chem.* **2009**, *48*, 1482. (d) Liu, C.-M.; Xiong, M.; Zhang, D.-Q.; Du, M.; Zhu, D.-B. *Dalton Trans.* **2009**, 5666. (e) Sun, D.; Ke, Y.; Collins, D. J.; Lorigan, G. A.; Zhou, H.-C. *Inorg. Chem.* **2007**, *46*, 2725. (f) Shu, M.; Tu, C.; Xu, W.; Jin, H.; Sun, J. *Cryst. Growth Des.* **2006**, *6*, 1890. (g) Bradshaw, D.; Claridge, J. B.; Cussen, E. J.; Prior, T. J.; Rosseinsky, M. J. *Acc. Chem. Res.* **2005**, *38*, 273. (h) Eubank, J. F.; Walsh, R. D.; Eddaoudi, M. *Chem. Commun.* **2005**, 2095. (i) Li, D.; Shi, W.-J.; Hou, L. *Inorg. Chem.* **2005**, *44*, 3907. (j) Prior, T.; Rosseinsky, M. *Inorg. Chem.* **2003**, *42*, 1564. (k) Keppert, C.; Prior, T.; Rosseinsky, M. *J. Am. Chem. Soc.* **2000**, *122*, 5158. (l) Yaghi, O. M.; Davis, C. E.; Li, G.; Li, H. *J. Am. Chem. Soc.* **1997**, *119*, 2861. (m) Abrahams, B.; Batten, S.; Hamit, H.; Hoskins, B.; Robson, R. *Chem. Commun.* **1996**, 1313.

(4) (a) Tang, Y.; Zhang, J.; Liu, W.-S.; Tan, M.-Y.; Yu, K.-B. *Polyhedron* **2005**, *24*, 1160. (b) Tang, S.-F.; Song, J.-L.; Li, X.-L.; Mao, J.-G. *Cryst. Growth Des.* **2006**, *6*, 2322. (c) Tang, Y.; Tang, K.-Z.; Liu, W.-S.; Tan, M.-Y. *Sci. Chin. Ser. B: Chem.* **2008**, *51*, 614.

(5) Guo, S.-P.; Guo, G.-C.; Wang, M.-S.; Zou, J.-P.; Zeng, H.-Y.; Cai, L.-Z.; Huang, J.-S. *Chem. Commun.* **2009**, 4366.

(6) Tian, Y.-C.; Liang, Y.-Q.; Ni, J.-Z. *Chin. Univ. Chem. J.* **1988**, *9*, 113.

(7) Farber, S.; Conley, R. T. *Syn. Commun.* **1994**, *4*, 243.

(8) Michio, K. *Bull. Chem. Soc. Jpn.* **1976**, *49*, 2679.

(9) (a) Sheldrick, G. M. *Acta Crystallogr. A.* **1990**, *46*, 467. (b) Sheldrick, G. M. *SHELXS-97, A Program for X-ray Crystal Structure Solution, and SHELXL-97, A Program for X-ray Structure Refinement*; Göttingen University: Germany, 1997.

(10) (a) Yi, C.-L.; Tang, Y.; Liu, W.-S.; Tan, M.-Y. *Inorg. Chem. Commun.* **2007**, *10*, 1505. (b) Liu, D.-Y.; Kou, Z.-Q.; Li, Y.-F.; Tang, K.-Z.; Tang, Y.; Liu, W.-S.; Tan, M.-Y. *Inorg. Chem. Commun.* **2009**, *12*, 461. (c) Wang, Q.; Tang, K.-Z.; Liu, W.-S.; Tang, Y.; Tan, M.-Y. *J. Solid State Chem.* **2009**, *182*, 3118.

(11) Spek, A. L. *PLATON*; Utrecht University: Utrecht, The Netherlands, 2003.

(12) Wells, A. F. *Three-dimensional Nets and Polyhedra*; Wiley-Interscience: New York, 1977.

(13) (a) Bu, X.-H.; Chen, W.; Du, M.; Biradha, K.; Wang, W.-Z.; Zhang, R.-H. *Inorg. Chem.* **2002**, *41*, 437. (b) Wang, Y.; Zhao, X.-Q.; Shi, W.; Cheng, P.; Liao, D.-Z.; Yan, S.-P. *Cryst. Growth Des.* **2009**, *9*, 2137.

(14) Öhrström, L.; Larsson, K. *Dalton Trans.* **2004**, 347.

(15) Albin, M.; Wright, R. R.; Horrocks, W. D. *Inorg. Chem.* **1985**, *24*, 4591.

(16) (a) Beeby, A.; Clarkson, I. M.; Eastoe, J.; Faulkner, S.; Warne, B. *Langmuir* **1997**, *13*, 5816. (b) Hebbink, G. A.; Klink, S. I.; Alink, P. G. B. O.; van Veggel, F. C. G. M. *Inorg. Chim. Acta* **2001**, *317*, 114. (c) Klonkowski, A. M.; Lis, S.; Hnatejko, Z.; Czarnobaj, K.; Pietraszkiewicz, M.; Elbanowski, M. *J. Alloys Compd.* **2000**, *300*−*301*, 55. (d) Okamoto, S.; Vyprachticky, D.; Furuya, H.; Abe, A.; Okamoto, Y. *Macromolecules* **1996**, *29*, 3511. (e) Zhu, L.; Tong, X.; Li, M.; Wang, E. *J. Phys. Chem. B* **2001**, *105*, 2461.

(17) Kirby, A. F.; Foster, D.; Richardson, F. S. *Chem. Phys. Lett.* **1983**, *95*, 507.

(18) Liu, W.-S.; Jiao, T.-Q.; Li, Y.-Z.; Liu, Q.-Z.; Tan, M.-Y.; Wang, H.; Wang, L.-F. *J. Am. Chem. Soc.* **2004**, *126*, 2280.

(19) (a) Fernandes, M.; de Zea Bermudez, V.; Sá Ferreira, R. A.; Carlos, L. D.; Charas, A.; Morgado, J.; Silva, M. M.; Smith, M. J. *Chem. Mater.* **2007**, *19*, 3892. (b) Su, Y.-G.; Li, L.-P.; Li, G.-S. *Chem. Mater.* **2008**, *20*, 6060. (c) Ma, Y.-F.; Wang, H.-P.; Liu, W.-S.; Wang, Q.; Xu, J.; Tang, Y. *J. Phy. Chem. B* **2009**, *113*, 14139.

(20) (a) Xu, H.; Wang, L.-H.; Zhu, X.-H.; Yin, K.; Zhong, G.-Y.; Hou, X.-Y.; Huang, W. *J. Phys. Chem. B* **2006**, *110*, 3023. (b) Ambili Raj, D. B.; Biju, S.; Reddy, M. L. P. *Inorg. Chem.* **2008**, *47*, 8091.

(21) Dawson, W.; Kropp, J.; Windsor, M. *J. Chem. Phys.* **1966**, *45*, 2410.

(22) He, P.; Wang, H.-H.; Liu, S.-G.; Shi, J.-X.; Wang, G.; Gong, M.-L. *Inorg. Chem.* **2009**, *48*, 11382.